Editors' Suggestion | Featured in Physics

Accelerating and Decelerating Space-Time Optical Wave Packets in Free Space

Murat Yessenov and Ayman F. Abouraddy
CREOL, The College of Optics and Photonics, University of Central Florida, Orlando, Florida 32816, USA

(Received 1 April 2020; accepted 30 October 2020; published 3 December 2020)

Although a plethora of techniques are now available for controlling the group velocity of an optical wave packet, there are very few options for creating accelerating or decelerating wave packets whose group velocity varies controllably along the propagation axis. Here we show that "space-time" wave packets in which each wavelength is associated with a prescribed spatial bandwidth enable the realization of optical acceleration and deceleration in free space. Endowing the field with precise spatiotemporal structure leads to group-velocity changes as high as $\sim c$ observed over a distance of $\sim$20 mm in free space, which represents a boost of at least $\sim$4 orders of magnitude over X waves and Airy pulses. The acceleration implemented is, in principle, independent of the initial group velocity, and we have verified this effect in both the subluminal and superluminal regimes.

DOI: 10.1103/PhysRevLett.125.233901

Acceleration refers to the departure from the condition of uniform motion along a straight line. With regards to *optical* fields, there have been to date only few realizations of acceleration. One example is that of Airy beams traveling in space along curved trajectories [1,2], whose acceleration has been recently exploited in inducing synchrotronlike radiation [3]; and another is axially accelerating wave packets. However, to date, attempts at observing accelerating optical wave packets have yielded only minute changes in the group velocity $\tilde{v}$. Airy pulses [4,5] have displayed $\Delta\tilde{v} \sim 10^{-4}c$ (where c is the speed of light in vacuum) over a distance of $\sim$75 cm in glass [6] (in contrast, Airy pulses in water displayed $\Delta\tilde{v}/\tilde{v} \approx 0.4$ [7]); and X waves [8,9] after introducing wave-front angular dispersion as proposed by Clerici *et al.* [10] have yielded accelerations of $\Delta\tilde{v} \sim 10^{-3}c$ and decelerations of $\Delta\tilde{v} \sim 3 \times 10^{-5}c$ over distances of $\sim$20 cm [11].

Synthesizing axially accelerating optical wave packets is predicated on the ability to control their group velocity. Slow- and fast-light systems can significantly vary the group velocity from c in *resonant* materials or structures [12] but *not* in free space. In a different context, anomalous group-velocity phenomena occur in the focal volume of focused ultrashort pulses [13], but we are interested here in wave packets that propagate for extended distances. A recent strategy for controlling $\tilde{v}$ in *free space* relies on endowing the field with precise spatiotemporal coupling. One approach known as the "flying focus" [14–16] exploits longitudinal chromatism to vary $\tilde{v}$ in the focal volume of a lens but whose spectrum evolves along the propagation axis. Another approach is that of "space-time" (ST) wave packets [17,18], in which each spatial frequency underlying the transverse spatial profile is coupled to a single wavelength [19–22], resulting in propagation invariance (diffraction-free and dispersion-free) [9,23,24] at an arbitrary $\tilde{v}$ [21,25–31]. Whereas X waves allow for group velocities that differ from c by only $\sim$0.1% in the paraxial regime [32–34], ST wave packets exhibit group velocities in the range from $30c$ to $-4c$ [28], *without* the narrow-band restrictions typical of slow- and fast-light systems [35]. Crucially, ST wave packets travel rigidly at a fixed $\tilde{v}$ in free space, including Airy ST wave packets that travel in a straight line [36]. A major rethinking of the spatiotemporal structure of ST wave packets is therefore required to produce axially *accelerating* counterparts.

Here we show that sculpting the spatiotemporal spectrum of ST wave packets enables the realization of record large axial acceleration. Rather than assigning each spatial frequency to a single wavelength as done previously for propagation-invariant ST wave packets [19,37], we assign a finite spatial spectrum whose central frequency *and* bandwidth vary in a precisely prescribed manner with the wavelength λ, which results in an axially encoded $\tilde{v}$. Using this approach, we observe group-velocity changes as large as $\Delta\tilde{v} \sim c$ over a distance of $\sim$20 mm, representing more than a 4-orders-of-magnitude boost over previous observations. We verify that acceleration and deceleration can each be realized in the subluminal *and* superluminal regimes. Such versatile capabilities in manipulating laser pulses may find applications ranging from nonlinear optics to plasma physics.

To synthesize ST wave packets, we make use of the setup depicted in Fig. 1. This arrangement is similar to that used previously in synthesizing wave packets of fixed $\tilde{v}$, but we extend it here to the synthesis of accelerating and decelerating ST wave packets. A pulsed laser beam from a mode-locked femtosecond Ti:sapphire oscillator is expanded spatially and directed to a 2D pulse synthesizer that introduces a judicious spatiotemporal spectral structure into the field via a 2D phase-only spatial light modulator

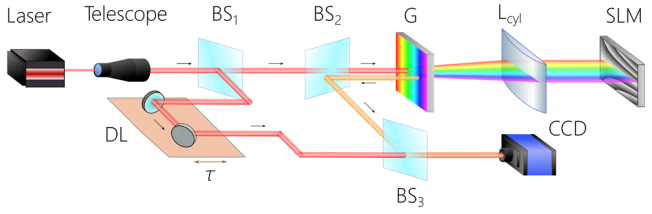

FIG. 1. Setup for the synthesis and characterization of accelerating ST wave packets. BS, beam splitter; G, diffraction grating; SLM, spatial light modulator; DL, delay line; L, lens.

(SLM) [38]. The synthesized ST wave packets travel at arbitrary prescribed $\tilde{v}$ (without violating relativistic causality [39–42]), which can be tuned by modifying the phase distribution Φ imparted to the spatially resolved spectrum by the SLM [28]. The spatiotemporal spectrum of the ST wave packet is recorded, and its time-averaged intensity in physical space is acquired to confirm diffraction-free propagation. The group velocity is measured interferometrically with respect to a short plane-wave reference pulse (see Supplemental Material [43], which includes Refs. [44,45]).

The concept of propagation-invariant ST wave packets can be elucidated by considering a single transverse coordinate x (field is uniform along y) and an axial coordinate z. The free-space dispersion relationship $k_x^2 + k_z^2 = (\omega/c)^2$ holds, which corresponds to the surface of the "light cone" [Fig. 2(a)], where k_x is the transverse component of the wave vector (or "spatial frequency"), k_z is the axial component, and ω is the angular frequency (or "temporal frequency"). The spectral support domain for a *propagation-invariant* ST wave packet is a 1D conic section at the intersection of the light cone with the spectral plane $\Omega = (k_z - k_o)c\tan\theta$, whose projection onto the $(k_z, \omega/c)$ plane is a straight line making an angle θ (the spectral tilt angle) with the k_z axis [Fig. 2(a)(i)]; here $\Omega = \omega - \omega_o$, ω_o is a fixed frequency, and $k_o = \omega_o/c$. The envelope of the field $E(x,z;t) = e^{i(k_o z - \omega_o t)}\psi(x,z;t)$ is [28]

$$\psi(x,z;t) = \int d\Omega \tilde{\psi}(\Omega) e^{i\{k_x x - \Omega[t-(z/\tilde{v})]\}} = \psi\left(x, 0; t - \frac{z}{\tilde{v}}\right), \tag{1}$$

corresponding to a wave packet traveling rigidly at a group velocity $\tilde{v} = \partial\omega/\partial k_z = c\tan\theta$, where $\tilde{\psi}(\Omega)$ is the Fourier

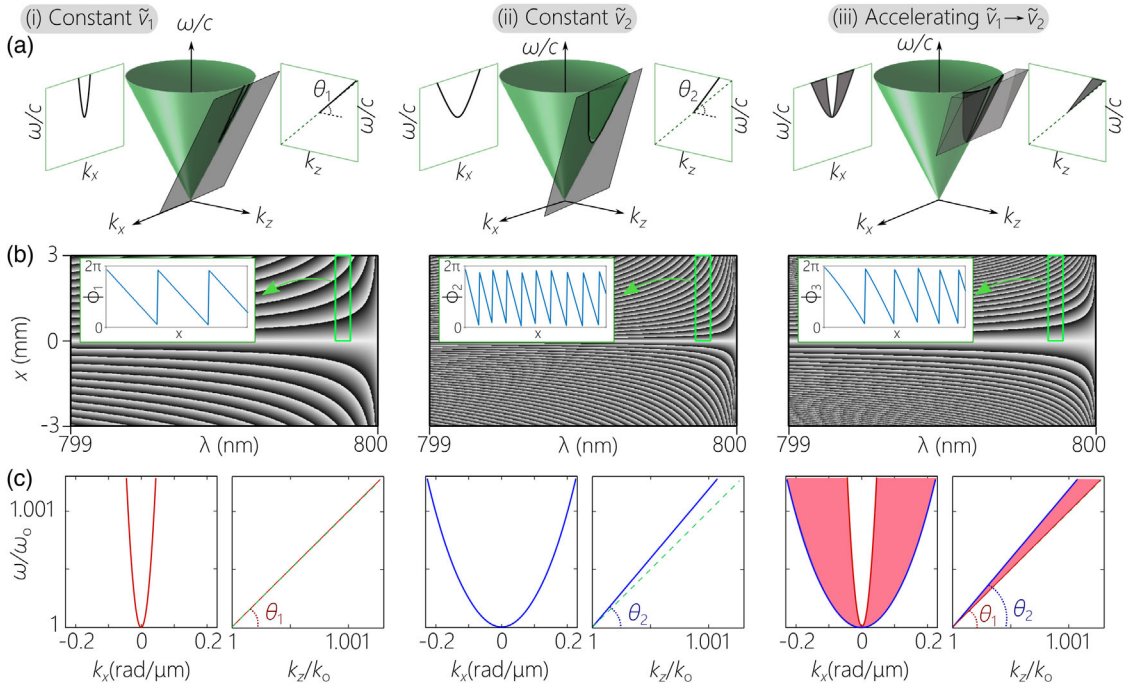

FIG. 2. (a) Representation of the spectral support domain of ST wave packets on the surface of the light cone. For propagation-invariant ST wave packets, the support domain is a conic section at the intersection of the light cone with a tilted spectral plane (here $\theta_1 = 45.2°$ and $\theta_2 = 47°$). For an accelerating ST wave packet, the support domain is the 2D area at the intersection of the light cone with a wedge-shaped volume bounded by two tilted spectral planes (θ_1 and θ_2). (b) Phase distribution Φ imparted by the SLM in Fig. 1 to the spectrally resolved wave front to produce ST wave packets of group velocity $\tilde{v}_1 = c\tan\theta_1$, group velocity $\tilde{v}_2 = c\tan\theta_2$, and acceleration $\tilde{v}_1 \to \tilde{v}_2$. Insets show the phases (modulo 2π) for a fixed temporal frequency (identified by the green box): $\Phi_1(x)$ and $\Phi_2(x)$ are linear phase distributions, each corresponding to a particular spatial frequency; $\Phi_3(x)$ is chirped between $\Phi_1(x)$ and $\Phi_2(x)$, thus corresponding to a finite spatial bandwidth. (c) Spectral projections onto the $(k_x, \omega/c)$ and $(k_z, \omega/c)$ planes for the ST wave packets in (a) and (b). The projections are 1D curves for constant-$\tilde{v}$ wave packets and 2D domains for accelerating wave packets. The dashed green line is the light line $k_z = \omega/c$.

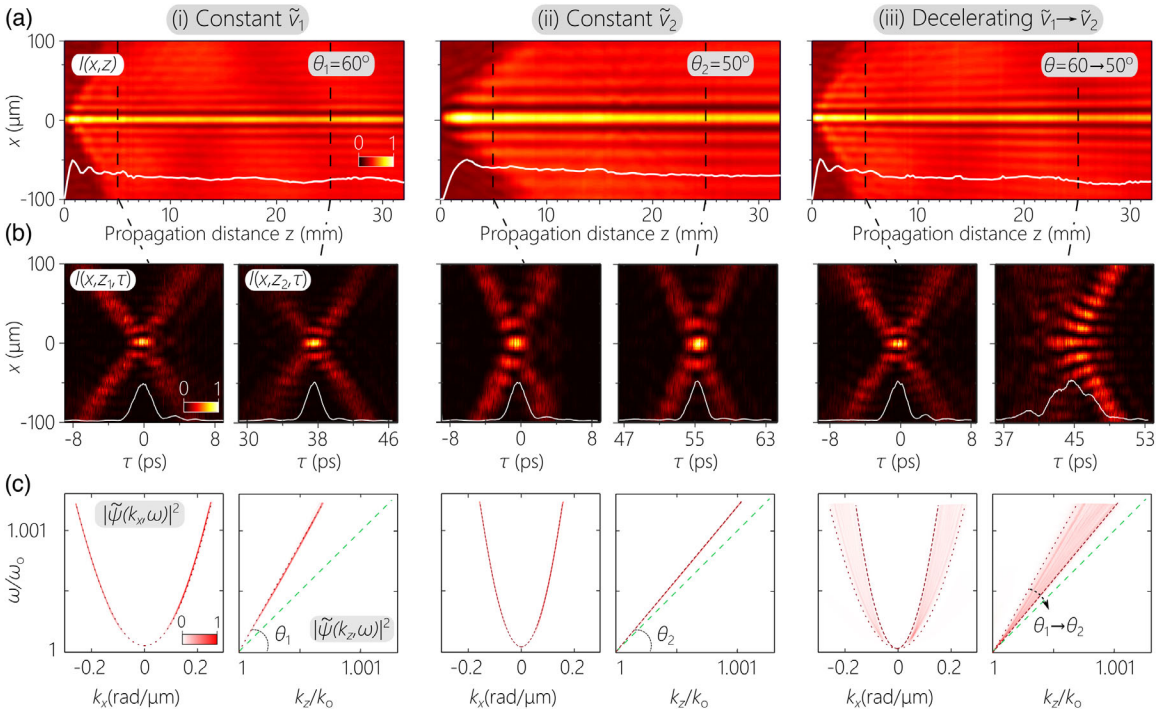

FIG. 3. (a) Measured axial evolution of the time-averaged intensity $I(x,z)$ for two constant-$\tilde{v}$ ST wave packets ($\tilde{v}_1 = c\tan\theta_1$ and $\tilde{v}_2 = c\tan\theta_2$) and a decelerating ST wave packet $\tilde{v}_1 \rightarrow \tilde{v}_2$ ($\tilde{v}_2 < \tilde{v}_1$); $\theta_1 = 60°$ and $\theta_2 = 50°$. The white line represents the normalized on-axis intensity evolution in z. (b) Measured spatiotemporal intensity profiles $I(x,z;\tau)$ of the ST wave packets at $z_1 = 5$ mm and $z_2 = 25$ mm, corresponding to the marked axial planes in (a). (c) Measured spatiotemporal spectral projections onto the (k_x,ω) and $(k_z,\omega/c)$ planes. The dotted red curves are theoretical predictions for the constant-$\tilde{v}$ ST wave packets, the dashed green line is the light line $k_z = \omega/c$, and $\lambda_o \approx 800$ nm (see Supplemental Material [43] for theoretical predictions).

transform of $\psi(0,0;t)$. Here k_x is *not* an independent variable but is instead related to Ω and θ through $k_x = \sqrt{2\omega_o\Omega(1-\tilde{n})}/c$, where $\tilde{n} = \cot\theta = c/\tilde{v}$ is the group index. Judicious design of the SLM phase distribution enables tuning θ [Figs. 2(b)(i) and 2(b)(ii)], resulting in ST wave packets with prescribed $\tilde{v}$ [28,29,46].

Consider two propagation-invariant ST wave packets of group velocities $\tilde{v}_1 = c\tan\theta_1$ and $\tilde{v}_2 = c\tan\theta_2$. Their spectral projections onto the $(k_z,\omega/c)$ plane are straight line making angles θ_1 or θ_2 with the k_z axis, respectively [Figs. 2(c)2(c)(i) and 2(c)(ii)]. We aim to produce a ST wave packet that accelerates from an initial value $\tilde{v}_1$ at $z = 0$ to $\tilde{v}_2$ at $z = L$: $\tilde{v}(z) = \tilde{v}_1 + (\tilde{v}_2 - \tilde{v}_1)z/L = c/\tilde{n}(z)$; i.e., the effective group index changes along z. To synthesize such a wave packet, we express the relationship between its spatial and temporal frequencies by the ansatz $k_x(\Omega,z) = \sqrt{2\omega_o\Omega[1-\tilde{n}(z)]}/c$. Consequently, each temporal frequency Ω is associated *not* with a single k_x (a condition necessary for propagation invariance) but instead with a *finite* Ω-dependent spatial bandwidth extending over the span $[k_x(\Omega,0), k_x(\Omega,L)]$. The envelope for the accelerating ST wave packet is given by

$$\psi(x,z;t) = \iint dk_x d\Omega \tilde{\psi}(\Omega)\tilde{h}(k_x,\Omega)e^{-i\Omega t}e^{i(k_x x + k_z z)}, \quad (2)$$

where $\tilde{h}(k_x,\Omega)$ imposes a Ω-dependent spatial spectrum. This configuration can be realized by *chirping* the SLM phase distribution to associate with each Ω the requisite span of spatial frequencies [Fig. 2(b)]. One can thus realize a ST wave packet whose $\tilde{v}$ changes between any two terminal values $\tilde{v}_1$ at $z = 0$ and $\tilde{v}_2$ at $z = L$ (accelerating $\tilde{v}_2 > \tilde{v}_1$ or decelerating $\tilde{v}_2 < \tilde{v}_1$). In this case, the spectral projection onto the $(k_x,\omega/c)$ plane is a 2D domain [Fig. 2(c)(iii)] bounded by the 1D curves corresponding to the ST wave packets of the terminal values $\tilde{v}_1$ and $\tilde{v}_2$. Similarly, the projection onto the $(k_z,\omega/c)$ plane is a 2D wedge-shaped domain bounded by straight lines making angles θ_1 and θ_2 with the k_z axis.

By implementing the appropriate SLM phase distributions, we obtain the measurement results plotted in Fig. 3. We set $\theta_1 = 60°$ ($\tilde{v}_1 \approx 1.73c$) and $\theta_2 = 50°$ ($\tilde{v}_2 \approx 1.19c$), corresponding to a decelerating wave packet. The intensity $I(x,z) = \int dt|\psi(x,z;t)|^2$ captured by a CCD camera scanned along z is provided in Fig. 3(a) for three ST wave packets: propagation-invariant wave packets traveling at $\tilde{v}_1$ and $\tilde{v}_2$, and a decelerating wave packet ($\tilde{v}_1 \rightarrow \tilde{v}_2$). The axial evolution of the intensity profile shows diffraction-free behavior for all three wave packets, with the axial range for the decelerating wave packet (48 mm) intermediate between the terminal constant-$\tilde{v}$ wave packets (36 mm for $\theta_1 = 60°$ and 145 mm for $\theta_2 = 50°$ [46]). Next,

time-resolved measurements are carried out along z to assess the group delay $\Delta\tau$ and local group velocity $\tilde{v}(z)$. We plot in Fig. 3(b) the spatiotemporal profile $I(x,z;\tau) = |\psi(x,z;\tau)|^2$ at two axial positions ($z = 5$ and 25 mm) for each wave packet. Over this distance, $\Delta\tau \sim 38$ ps and $\Delta\tau \sim 55$ ps for the ST wave packets traveling at $\tilde{v}_1$ and $\tilde{v}_2$, respectively, which are consistent with $\Delta z/\tilde{v}_1$ and $\Delta z/\tilde{v}_2$ ($\Delta z = 20$ mm); while $\Delta\tau$ for the decelerating wave packet has an intermediate value. The measured spectral projections onto the $(k_x, \omega/c)$ and $(k_z, \omega/c)$ planes confirm that the synthesized ST wave packets reproduce the target spectral structure. The spectral projection onto the $(k_x, \omega/c)$ plane for the decelerating wave packet is a 2D domain bounded by the 1D curves for the constant-$\tilde{v}$ limits, and the projection onto the $(k_z, \omega/c)$ plane is a wedge-shaped domain extending between 60° and 50°.

For a constant-$\tilde{v}$ ST wave packet, the propagation distance is $L_{\max} = (c/\delta\omega)(1/|1 - \cot\theta|)$, where the spectral uncertainty $\delta\omega$ (which is typically much smaller than the full temporal spectral bandwidth) is the unavoidable "fuzziness" in the association between each k_x and ω (due in our setup mainly to the spectral resolution of the diffraction grating) [46]. In the case of accelerating ST wave packets, because we no longer have a one-to-one relationship between k_x and ω, pulse dispersion is introduced [47]; see Fig. 3(b)(iii).

To establish that the synthesized ST wave packets accelerate and decelerate at the prescribed rates, we plot in Fig. 4 the measured $\Delta\tau$ (with respect to a frame moving at the initial speed $\tilde{v}_1$) obtained at 5-mm axial intervals and the estimated $\tilde{v}(z)$ for accelerating and decelerating ST wave packets. Therefore, $\Delta\tau$ at $z = 0$ is zero in all cases (and remains zero for constant-$\tilde{v}$ wave packets), and subsequently $\Delta\tau > 0$ for decelerating wave packets and $\Delta\tau < 0$ for accelerating ones. Moreover, the data in Fig. 4 serve also to confirm that acceleration can be realized in both the subluminal ($\theta < 45°$) and superluminal ($\theta > 45°$) regimes [37]. In all cases, we find that $\Delta\tau$ has a *parabolic* dependence and $\tilde{v}(z)$ a *linear* dependence on z, as expected for linearly accelerating wave packets.

We first present in Fig. 4(a) measurements for *subluminal* decelerating $\Delta\tilde{v} = -0.07c$ ($\theta_1 = 40° \to \theta_2 = 30°$, $\tilde{v}_1 = 0.84c \to \tilde{v}_2 = 0.58c$) and accelerating $\Delta\tilde{v} = 0.09c$ ($30° \to 43°$, $0.58c \to 0.93c$) wave packets. Next, we present in Fig. 4(b) measurements for *superluminal* decelerating $\Delta\tilde{v} = -0.19c$ ($70° \to 50°$, $2.75c \to 1.19c$) and accelerating $\Delta\tilde{v} = 0.24c$ ($50° \to 70°$, $1.19c \to 2.75c$) wave packets. Finally, Fig. 4(c) provides further measurements for superluminal decelerating $\Delta\tilde{v} = -1.18c$ ($82° \to 70°$, $7.12c \to 2.74c$) and accelerating $\Delta\tilde{v} = 0.56c$ ($70° \to 82°$, $2.74c \to 7.12c$) wave packets, which exceeds by 4 orders of magnitude previously reported measurements [6,11].

The synthesized accelerating ST wave packets fall short of the targeted terminal group velocities $\tilde{v}_2$ due to the finite

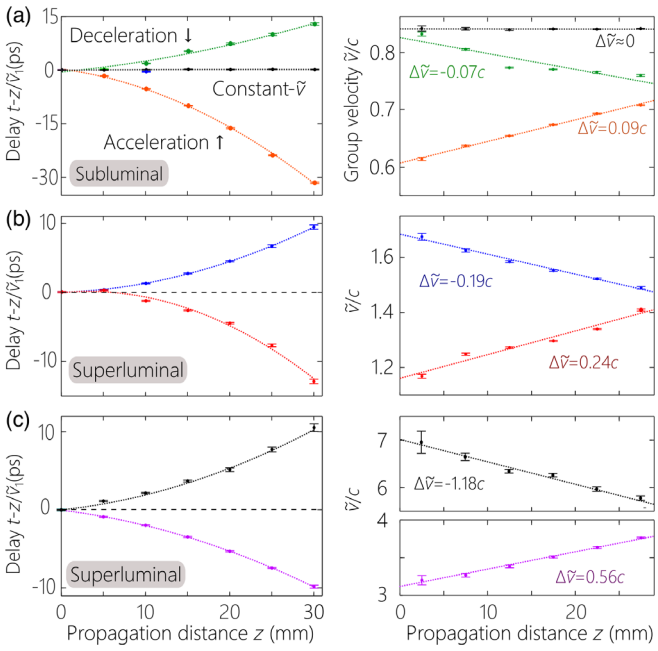

FIG. 4. (a) Measured group delays (left) with respect to a pulse traveling at the initial group velocity $\tilde{v}_1$ at $z = 0$ and group velocities (right). We plot data for accelerating and decelerating subluminal ST wave packets over a propagation distance of 30 mm and also plot for comparison data for a constant-$\tilde{v}$ ST wave packet at the initial group velocity $\tilde{v}_1$. (b) The same as (a) for superluminal ST wave packets. (c) The same as (b) for superluminal ST wave packets with large acceleration and deceleration. Points are the measured data, and the dotted curves are theoretical fits (quadratic for the delays, linear for the group velocities).

pixel size and number of pixels of the SLM that limit the achievable chirping rate. This is associated with pulse distortion in the accelerating ST wave packets (compared to the rigid propagation of the constant-$\tilde{v}$ wave packets); see Fig. 3(c) confirmed by the simulations provided in Supplemental Material [43]. This limitation can be alleviated by utilizing lithographically inscribed phase plates of higher spatial resolution and larger size [48–51].

The strategy outlined here for the synthesis of accelerating and decelerating optical wave packets represents a fundamental departure from previous approaches, such as Airy pulses or wavefront-modulated X waves. Our approach is quite general, does not require a resonant material or structure and, thus, has no fundamental limit on the exploitable bandwidth; it does not require utilizing a dispersive medium; and it can be utilized to produce other axial acceleration profiles such as sublinear or superlinear acceleration or combined acceleration *and* deceleration over prescribed axial domains.

It has been shown that accelerating fields can help selectively manipulate nonlinear frequency conversion processes when combined with quasi-phase-matching schemes [52]. The results here realize such acceleration

in a versatile configuration and may also lead to new sources of radiation [3] and acceleration of charged particles [53], in addition to enhancements in nonlinear optics [52,54,55] and plasma interactions [56]. By synthesizing multiple copropagating ST wave packets in the same or different spectral windows [35], copropagating pulses can be arranged to collide once or multiple times over the course of their propagation. Finally, although ST wave packets can be coupled into planar waveguides [57], more research is needed to ascertain whether they can be coupled efficiently into optical fibers.

In conclusion, we have synthesized a new class of ST wave packets that (i) accelerate or decelerate in free space; (ii) can be realized in both the subluminal and superluminal regimes; (iii) exhibit record changes in the group velocity extending to $\Delta\tilde{v} \sim 1.2c$ over a propagation distance of $\sim$20 mm; and (iv) all by virtue of their spatiotemporal spectral structure in which each wavelength is associated with a prescribed spatial spectrum whose center and bandwidth are wavelength dependent. The achieved accelerations are at least 4 orders of magnitude larger than previously reported.

This work was funded by the U.S. Office of Naval Research Contract No. N00014-17-1-2458.

[1] G. A. Siviloglou and D. N. Christodoulides, Accelerating finite energy Airy beams, Opt. Lett. **32**, 979 (2007).
[2] N. K. Efremidis, Z. Chen, M. Segev, and D. N. Christodoulides, Airy beams and accelerating waves: An overview of recent advances, Optica **6**, 686 (2019).
[3] M. Henstridge, C. Pfeiffer, D. Wang, A. Boltasseva, V. M. Shalaev, A. Grbic, and R. Merlin, Synchrotron radiation from an accelerating light pulse, Science **362**, 439 (2018).
[4] D. Abdollahpour, S. Suntsov, D. G. Papazoglou, and S. Tzortzakis, Spatiotemporal Airy Light Bullets in the Linear and Nonlinear Regimes, Phys. Rev. Lett. **105**, 253901 (2010).
[5] I. Kaminer, Y. Lumer, M. Segev, and D. N. Christodoulides, Causality effects on accelerating light pulses, Opt. Express **19**, 23132 (2011).
[6] A. Chong, W. H. Renninger, D. N. Christodoulides, and F. W. Wise, AiryBessel wave packets as versatile linear light bullets, Nat. Photonics **4**, 103 (2010).
[7] S. Fu, Y. Tsur, J. Zhou, L. Shemer, and A. Arie, Propagation Dynamics of Airy Water-Wave Pulses, Phys. Rev. Lett. **115**, 034501 (2015).
[8] J.-Y. Lu and J. F. Greenleaf, Nondiffracting x waves—Exact solutions to free-space scalar wave equation and their finite aperture realizations, IEEE Trans. Ultrason. Ferroelectr. Freq. Control **39**, 19 (1992).
[9] P. Saari and K. Reivelt, Evidence of X-Shaped Propagation-Invariant Localized Light Waves, Phys. Rev. Lett. **79**, 4135 (1997).
[10] M. Clerici, D. Faccio, A. Lotti, E. Rubino, O. Jedrkiewicz, J. Biegert, and P. D. Trapani, Finite-energy, accelerating Bessel pulses, Opt. Express **16**, 19807 (2008).
[11] H. Valtna-Lukner, P. Bowlan, M. Lõhmus, P. Piksarv, R. Trebino, and P. Saari, Direct spatiotemporal measurements of accelerating ultrashort Bessel-type light bullets, Opt. Express **17**, 14948 (2009).
[12] R. W. Boyd and D. J. Gauthier, Controlling the velocity of light pulses, Science **326**, 1074 (2009).
[13] M. A. Porras, I. Gonzalo, and A. Mondello, Pulsed light beams in vacuum with superluminal and negative group velocities, Phys. Rev. E **67**, 066604 (2003).
[14] A. Sainte-Marie, O. Gobert, and F. Quéré, Controlling the velocity of ultrashort light pulses in vacuum through spatiotemporal couplings, Optica **4**, 1298 (2017).
[15] D. H. Froula, D. Turnbull, A. S. Davies, T. J. Kessler, D. Haberberger, J. P. Palastro, S.-W. Bahk, I. A. Begishev, R. Boni, S. Bucht, J. Katz, and J. L. Shaw, Spatiotemporal control of laser intensity, Nat. Photonics **12**, 262 (2018).
[16] S. W. Jolly, O. Gobert, A. Jeandet, and F. Quéré, Controlling the velocity of a femtosecond laser pulse using refractive lenses, Opt. Express **28**, 4888 (2020).
[17] H. E. Kondakci and A. F. Abouraddy, Diffraction-free pulsed optical beams via space-time correlations, Opt. Express **24**, 28659 (2016).
[18] H. E. Kondakci and A. F. Abouraddy, Diffraction-free space-time light sheets, Nat. Photonics **11**, 733 (2017).
[19] R. Donnelly and R. Ziolkowski, Designing localized waves, Proc. R. Soc. A **440**, 541 (1993).
[20] P. Saari and K. Reivelt, Generation and classification of localized waves by Lorentz transformations in Fourier space, Phys. Rev. E **69**, 036612 (2004).
[21] S. Longhi, Gaussian pulsed beams with arbitrary speed, Opt. Express **12**, 935 (2004).
[22] K. J. Parker and M. A. Alonso, The longitudinal iso-phase condition and needle pulses, Opt. Express **24**, 28669 (2016).
[23] J. Turunen and A. T. Friberg, Propagation-invariant optical fields, Prog. Opt. **54**, 1 (2010).
[24] *Non-Diffracting Waves*, edited by H. E. Hernández-Figueroa, E. Recami, and M. Zamboni-Rached (Wiley-VCH, New York, 2014).
[25] J. Salo and M. M. Salomaa, Diffraction-free pulses at arbitrary speeds, J. Opt. A **3**, 366 (2001).
[26] C. J. Zapata-Rodríguez and M. A. Porras, X-wave bullets with negative group velocity in vacuum, Opt. Lett. **31**, 3532 (2006).
[27] L. J. Wong and I. Kaminer, Ultrashort tilted-pulsefront pulses and nonparaxial tilted-phase-front beams, ACS Photonics **4**, 2257 (2017).
[28] H. E. Kondakci and A. F. Abouraddy, Optical space-time wave packets of arbitrary group velocity in free space, Nat. Commun. **10**, 929 (2019).
[29] B. Bhaduri, M. Yessenov, and A. F. Abouraddy, Space-time wave packets that travel in optical materials at the speed of light in vacuum, Optica **6**, 139 (2019).
[30] B. Bhaduri, M. Yessenov, and A. F. Abouraddy, Anomalous refraction of optical spacetime wave packets, Nat. Photonics **14**, 416 (2020).
[31] K. L. Schepler, M. Yessenov, Y. Zhiyenbayev, and A. F. Abouraddy, Space-time surface plasmon polaritons: A new propagation-invariant surface wave packet, arXiv:2003.02105.

[32] P. Bowlan, H. Valtna-Lukner, M. Lõhmus, P. Piksarv, P. Saari, and R. Trebino, Measuring the spatiotemporal field of ultrashort Bessel-X pulses, Opt. Lett. **34**, 2276 (2009).
[33] K. B. Kuntz, B. Braverman, S. H. Youn, M. Lobino, E. M. Pessina, and A. I. Lvovsky, Spatial and temporal characterization of a bessel beam produced using a conical mirror, Phys. Rev. A **79**, 043802 (2009).
[34] F. Bonaretti, D. Faccio, M. Clerici, J. Biegert, and P. Di Trapani, Spatiotemporal amplitude and phase retrieval of Bessel-X pulses using a Hartmann-Shack sensor, Opt. Express **17**, 9804 (2009).
[35] M. Yessenov, B. Bhaduri, P. J. Delfyett, and A. F. Abouraddy, Free-space optical delay line using space-time wave packets, Nat. Commun. **11**, 5782 (2020).
[36] H. E. Kondakci and A. F. Abouraddy, Airy Wavepackets Accelerating in Space-Time, Phys. Rev. Lett. **120**, 163901 (2018).
[37] M. Yessenov, B. Bhaduri, H. E. Kondakci, and A. F. Abouraddy, Classification of propagation-invariant space-time light-sheets in free space: Theory and experiments, Phys. Rev. A **99**, 023856 (2019).
[38] A. M. Weiner, *Ultrafast Optics* (John Wiley & Sons, Inc., New York, 2009).
[39] A. M. Shaarawi, R. W. Ziolkowski, and I. M. Besieris, On the evanescent fields and the causality of focus wave modes, J. Math. Phys. (N.Y.) **36**, 5565 (1995).
[40] P. Saari, Reexamination of group velocities of structured light pulses, Phys. Rev. A **97**, 063824 (2018).
[41] P. Saari, O. Rebane, and I. Besieris, Reexamination of energy flow velocities of non-diffracting localized waves, Phys. Rev. A **100**, 013849 (2019).
[42] P. Saari and I. Besieris, Reactive energy in nondiffracting localized waves, Phys. Rev. A **101**, 023812 (2020).
[43] See Supplemental Material at http://link.aps.org/supplemental/10.1103/PhysRevLett.125.233901 for a detailed description of the experimental configuration and procedure, and for theoretical predictions corresponding to the measurements presented here.
[44] M. Yessenov, B. Bhaduri, H. E. Kondakci, and A. F. Abouraddy, Weaving the rainbow: Space-time optical wave packets, Opt. Photonics News **30**, 34 (2019).
[45] M. S. Wartak, *Computational Photonics: An Introduction with MATLAB* (Cambridge University Press, Cambridge, England, 2013).
[46] M. Yessenov, B. Bhaduri, L. Mach, D. Mardani, H. E. Kondakci, M. A. Alonso, G. A. Atia, and A. F. Abouraddy, What is the maximum differential group delay achievable by a space-time wave packet in free space?, Opt. Express **27**, 12443 (2019).
[47] H. E. Kondakci, M. A. Alonso, and A. F. Abouraddy, Classical entanglement underpins the propagation invariance of space-time wave packets, Opt. Lett. **44**, 2645 (2019).
[48] P. Wang, J. A. Dominguez-Caballero, D. J. Friedman, and R. Menon, A new class of multi-bandgap high-efficiency photovoltaics enabled by broadband diffractive optics, Prog. Photovoltaics **23**, 1073 (2015).
[49] H. E. Kondakci, M. Yessenov, M. Meem, D. Reyes, D. Thul, S. R. Fairchild, M. Richardson, R. Menon, and A. F. Abouraddy, Synthesizing broadband propagation-invariant space-time wave packets using transmissive phase plates, Opt. Express **26**, 13628 (2018).
[50] B. Bhaduri, M. Yessenov, D. Reyes, J. Pena, M. Meem, S. R. Fairchild, R. Menon, M. C. Richardson, and A. F. Abouraddy, Broadband space-time wave packets propagating for 70 m, Opt. Lett. **44**, 2073 (2019).
[51] M. Yessenov, B. Bhaduri, H. E. Kondakci, M. Meem, R. Menon, and A. F. Abouraddy, Non-diffracting broadband incoherent space-time fields, Optica **6**, 598 (2019).
[52] A. Bahabad, M. M. Murnane, and H. C. Kapteyn, Manipulating nonlinear optical processes with accelerating light beams, Phys. Rev. A **84**, 033819 (2011).
[53] S. W. Jolly, Influence of Longitudinal Chromatism on Vacuum Acceleration by Intense Radially Polarized Laser Beams, Opt. Lett. **44**, 1833 (2019).
[54] Y. Hu, Z. Li, B. Wetzel, R. Morandotti, Z. Chen, and J. Xu, Cherenkov radiation control via self-accelerating wavepackets, Sci. Rep. **7**, 8695 (2017).
[55] P. Jia, Z. Li, Y. Hu, Z. Chen, and J. Xu, Visualizing a Nonlinear Response in a Schrödinger Wave, Phys. Rev. Lett. **123**, 234101 (2019).
[56] A. J. Howard, D. Turnbull, A. S. Davies, P. Franke, D. H. Froula, and J. P. Palastro, Photon Acceleration in a Flying Focus, Phys. Rev. Lett. **123**, 124801 (2019).
[57] A. Shiri, M. Yessenov, S. Webster, K. L. Schepler, and A. F. Abouraddy, Hybrid guided space-time optical modes in unpatterned films, arXiv:2001.01991.